

Constraints on the Physical Association between ICECAT1 Neutrinos and Fast Radio Bursts Using the Second CHIME/FRB Catalogue

HIROTO MASAOKA ^{1,2}, TETSUYA HASHIMOTO ³, SHOTARO YAMASAKI ³, YUHEI IWATA ^{2,4}, TOMOKI WADA ^{3,5,6},
TOMOTSUGU GOTO ⁷, SHINTARO YOSHIURA ⁸, KAZUAKI HASHIYAMA ², MAREKI HONMA ^{1,2,8}, TAKUYA AKAHORI ⁸,
AND KOHEI KURAHARA ⁹

¹Department of Astronomy, School of Science, The University of Tokyo, 7-3-1 Hongo, Bunkyo-ku, Tokyo 113-0033, Japan

²Mizusawa VLBI Observatory, National Astronomical Observatory of Japan, 1-2-2 Mizusawa-Hoshigaoka, Oshu, Iwate 023-0861, Japan

³Department of Physics, National Chung Hsing University, No. 145, Xingda Rd., South Dist., Taichung, 40227, Taiwan

⁴Astronomical Science Program, Graduate Institute for Advanced Studies, SOKENDAI, 2-21-1 Osawa, Mitaka, Tokyo 181-8588, Japan

⁵Frontier Research Institute for Interdisciplinary Sciences, Tohoku University, Sendai, Miyagi 980-8578, Japan

⁶Astronomical Institute, Graduate School of Science, Tohoku University, Sendai, Miyagi 980-8578, Japan

⁷Institute of Astronomy, National Tsing Hua University, No. 101, Section 2, Kuang-Fu Road, Hsinchu City 30013, Taiwan

⁸Mizusawa VLBI Observatory, National Astronomical Observatory of Japan, 2-21-1 Osawa, Mitaka, Tokyo 181-8588, Japan

⁹Institute for the Origin of Particles and the Universe (KMI), Nagoya University, Furo-cho, Chikusa-ku, Nagoya, Aichi 464-8601, Japan

Submitted to ApJ

ABSTRACT

We present a search for neutrino counterparts to fast radio bursts (FRBs) using temporal and spatial cross-matching between the Second CHIME/FRB catalogue and the IceCube high-energy alert-track catalogue ICECAT1. Because current FRB–neutrino models do not provide a unique consensus on emission ordering, our primary significance test adopts a two-sided, order-agnostic temporal hypothesis. The analysis accounts for declination-dependent CHIME/FRB exposure and the look-elsewhere effect across multiple trials. No statistically significant FRB–neutrino association is found. The most significant pair is FRB 20190630C–IC 190629A, with a post-trial probability of $p = 0.076$ (1.43σ), consistent with a chance coincidence. Within our statistical framework, a detectable physical association would require a time offset shorter than ~ 256 s at 3σ or ~ 63 ms at 5σ . Using a population-level stacking analysis, we derive 90% upper limits on the neutrino-to-radio luminosity ratio of FRBs, $\xi \lesssim 10^8 - 10^{11}$ for neutrino power-law spectral indices $\gamma = 1.0 - 3.0$. These limits improve upon previous constraints by approximately two orders of magnitude and represent the most stringent bounds from FRB–neutrino coincidence searches to date. Although the current limits remain above the predictions of most magnetar-based models, they begin to constrain scenarios involving exceptionally efficient hadronic energy dissipation.

Keywords: Radio bursts (1339) — Radio transient sources (2008) — Neutrino astronomy (1100) — High Energy astrophysics (739)

1. INTRODUCTION

Fast Radio Bursts (FRBs) are extraordinarily powerful radio transients characterized by a brightness temperature of $\sim 10^{36}$ K, millisecond durations, and large dispersion measures (DM), indicating their origin from cosmological distances (e.g., D. R. Lorimer et al. 2007).

Despite significant observations and theoretical progress (e.g. E. Petroff et al. 2022), the progenitors and mechanisms of FRBs remain elusive. To distinguish between various FRB models proposed so far (e.g., E. Platts et al. 2019), acquiring additional insights through multi-wavelength and multi-messenger observations is essential. For example, the detection of FRB 20200428D (The CHIME/FRB Collaboration et al. 2020a; C. D. Bochenek et al. 2020) and its association with hard X-ray bursts (S. Mereghetti et al. 2020; C. K. Li et al.

2021; A. Ridnaia et al. 2021; M. Tavani et al. 2021; X. Li et al. 2022) strongly supports magnetars as plausible FRB progenitors.

Despite extensive follow-up efforts (e.g. S. Yamasaki et al. 2016; L. Nicastro et al. 2021; B. Zhang 2024), identifying high-energy counterparts to extragalactic FRBs remains challenging. A 15–50 keV GRB-like signal lasting for 300 s was tentatively linked to FRB 20131104 at 3.2σ significance (J. J. DeLaunay et al. 2016). A potential association between the binary neutron star merger GW 190425 (B. P. Abbott et al. 2020) and the non-repeating FRB 20190425A was reported with a chance probability of 0.0052 (2.8σ) (A. Moroianu et al. 2022). Additionally, recent theoretical work has proposed high energy (HE, ≥ 100 TeV) neutrino emission in the TeV–PeV range associated with FRBs via photo-hadronic interactions (B. D. Metzger et al. 2020; Y. Qu & B. Zhang 2022; J. Shimoda & T. Wada 2024), with different delay structures and possible emission orderings (FRB-before-neutrino or FRB-after-neutrino). However, despite multiple searches using ANTARES and IceCube data, no statistically significant neutrino counterparts to FRBs have been identified. This non-detection likely reflects several practical limitations: limited temporal overlap between FRB and neutrino detections, heterogeneous FRB samples compiled from different instruments, and reduced statistical power in joint temporal and spatial coincidence tests. In small-sample studies, temporal and spatial coincidence criteria were applied simultaneously but with limited event statistics (S. Fahey et al. 2017; A. Albert et al. 2018; M. G. Aartsen et al. 2018, 2020; R. Abbasi et al. 2023a), whereas the larger-sample studies emphasized either temporal or spatial correlations (S. Desai 2022; J.-W. Luo & B. Zhang 2024). This methodological split has made it difficult to establish a robust physical FRB–neutrino connection.

More generally, the identification of astrophysical neutrino sources is challenged by substantial atmospheric background noise and limited directional accuracy, which weakens source-association significance between neutrino detections and their potential sources (e.g. S. V. Troitsky 2021; A. Sharma 2024). Despite the hundreds of HE neutrino detections by the IceCube neutrino observatory in the TeV–PeV energy range (R. Abbasi et al. 2023b), only a small number of promising candidate sources have been identified. In 2018, the IceCube collaboration reported an association between a HE neutrino event, IC 170922A, and a gamma-ray flare from blazar TXS 0506+056, with a significance of 3σ (M. Aartsen et al. 2018a). They also reported another association between the blazar TXS 0506+056 and a neutrino flare in the same direction

between 2014 September and 2015 March, during which TXS 0506+056 was not at a gamma-ray flaring state (M. Aartsen et al. 2018b). This association significance was 2.4σ (IceCube Collaboration 2021; W. Luszczyk 2023). In 2022, the IceCube collaboration found evidence of neutrino emission from a type 2 Seyfert galaxy, NGC 1068, with a significance of 4.2σ (R. Abbasi et al. 2022). Both findings have been associated with the detection of multiple neutrinos across a range of energies. In contrast, the significance of other candidate sources, typically identified based only on a single neutrino detection, is weaker (M. Bustamante et al. 2024, See Sec. VI). These previous works illustrate that modest-significance ($\sim 2\text{--}4\sigma$) associations can provide useful exploratory clues in multi-messenger astronomy, but establishing a physical source class requires additional events and independent confirmation.

In this paper, aiming to search for neutrino counterparts to FRBs, we investigate temporal and spatial coincidences between high-energy neutrino alerts from ICECAT1 (R. Abbasi et al. 2023b) and FRBs from the Second CHIME/FRB Catalogue (F. Collaboration et al. 2026), with supplementary checks using the first CHIME/FRB baseband catalogue (The CHIME/FRB Collaboration et al. 2024). A key distinction of this work compared to previous studies (S. Fahey et al. 2017; A. Albert et al. 2018; M. G. Aartsen et al. 2018, 2020; R. Abbasi et al. 2023a; S. Desai 2022; J.-W. Luo & B. Zhang 2024) is that we apply a joint temporal–spatial framework to a homogeneous FRB sample over a well-defined overlap period (2018 July 25–2020 December 31). This design enables a uniform and statistically robust search compared with earlier studies. By combining temporal and spatial information within a framework, we provide a more consistent test of potential FRB–neutrino associations and derive improved constraints on neutrino emission from FRBs

This paper is structured as follows: In Section 2, we present the initial temporal and spatial cross-match to identify potential FRB–neutrino associations. In Section 3, we evaluate the statistical significance of the candidate pairs, and derive upper limits on the detectable FRB–neutrino time offset in this data set. In Section 4, we derive upper limits on the neutrino-to-radio luminosity ratio from the non-detection. In Section 5, we discuss the implications for FRB–neutrino connections in the broader high-energy neutrino context and summarize our conclusions. Throughout, we assume a standard Λ CDM cosmology ($\Omega_m = 0.3111$, $\Omega_\Lambda = 0.6889$, $\Omega_b = 0.04897$, $h = 0.6766$).

2. INITIAL SEARCH FOR POTENTIAL NEUTRINO-FRB ASSOCIATIONS

Initially, we perform a comprehensive search for temporal and spatial coincidences between FRBs and neutrino events across the full overlapping time coverage of the two datasets. For each neutrino event, we identify FRBs that occur within the 90% localization uncertainty region. No a priori constraint is imposed on the temporal separation between the two events at this stage.

For illustrative purposes, Table 1 lists candidate pairs with temporal separations smaller than 30 days. This presentation window is adopted only to highlight representative cases and does not constitute a physical or statistical assumption about the expected FRB–neutrino delay. In particular, theoretical models typically predict much shorter timescales for FRB-associated neutrino emission (e.g., $\lesssim 1000$ s; B. D. Metzger et al. 2020). Our search strategy therefore remains agnostic with respect to the emission timescale and is designed to capture any potential associations present in the data.

The Second CHIME/FRB Catalogue contains 4539 FRBs observed between 2018 July 25 and 2023 September 15, originating from 3641 unique sources (F. Collaboration et al. 2026). In our analysis, to maintain consistency with the time overlap between the first-year CHIME/FRB observing window and the ICECAT1 event set used here, we focus on the 1823 FRBs (1562 apparently non-repeating FRBs) detected between 2018 July 25 and 2020 December 31, corresponding to the first-year subset of the Second CHIME/FRB Catalogue. We cross-match these events with 73 neutrino alerts from the ICECAT1 catalogue (R. Abbasi et al. 2023b) over the same time interval. Note that we treat an FRB with multiple sub-bursts as a single event.

In this initial search, we identify 12 out of 1823 FRBs ($\sim 0.66\%$) that are coincident with neutrino events within a symmetric ± 30 days time window and satisfy the spatial coincidence criterion (see Table 1 and Table 2). One notable example is FRB 20190630C, which occurred 0.93 days (22 hours) after the neutrino event IC 190629A within the positional uncertainty region. The statistical significance of this candidate is evaluated in the following section.

3. SIGNIFICANCE ANALYSIS

In this section, we evaluate the statistical significance of the candidate association between FRB 20190630C and IC 190629A, as well as the overall FRB–neutrino associations. We define an FRB–neutrino association for a given neutrino event ν_i as the occurrence of at least one non-repeating FRB that satisfies both of the following conditions: (i) it falls within a two-sided temporal win-

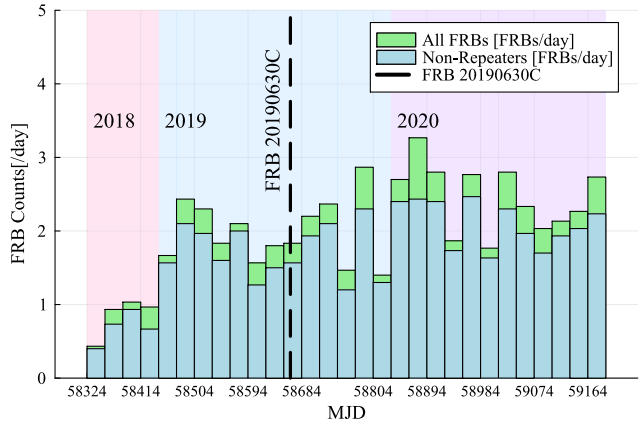


Figure 1. The daily FRB detection rate derived from the Second CHIME/FRB Catalogue. The histogram shows the number of FRBs detected per day, binned in 30-day intervals. FRB 20190630C is shown as a representative example.

now before and after the neutrino detection, and (ii) it lies within the 90% localization region of ν_i . Under the null hypothesis that FRBs and neutrino events are unrelated, we evaluate, for each neutrino event, the probability that such an association arises by chance. We then combine the results from all neutrino events to derive a trial-corrected probability, which we use to quantify the statistical significance of any apparent association.

Following A. Moroianu et al. (2022), we decompose the chance-coincidence probability into a temporal term and a spatial term. The temporal term corresponds to the probability that CHIME/FRB detects at least one non-repeating FRB within a specified two-sided time window before and after ν_i (Section 3.1), while the spatial term represents the probability that a detected FRB falls within the 90% localization region of ν_i (Section 3.2). This analysis accounts for the declination-dependent observational exposure of CHIME/FRB. We then combine these terms and apply a trial correction across all neutrino alerts to obtain the final probability used to compute the significance (Section 3.3).

Although several FRB–neutrino emission models have been proposed (e.g., B. D. Metzger et al. 2020; Y. Qu & B. Zhang 2022), the relative emission order between FRBs and neutrinos remains unconstrained. We therefore adopt a two-sided temporal hypothesis (i.e., without assuming any specific emission ordering) as the primary analysis, and additionally consider one-sided hypotheses (FRB-after-neutrino and FRB-before-neutrino) for comparison.

3.1. Probability of a chance temporal coincidence P_T

The probability of a chance temporal coincidence, P_T , is defined as the Poisson probability of a random FRB

Table 1. FRB–neutrino candidate pairs identified in the initial cross-match

CHIME FRB	MJD	RA	Dec	DM	Fluence	Coincident Neutrino	Time Gap
		(deg)	(deg)	(pc cm ⁻³)	(Jy ms)		(day)
FRB 20190409A	58582.007	79.62 ± 0.20	6.72 ± 0.27	1791.87	8.52	IC 190317A	22.175
FRB 20190609A	58643.115	347.92 ± 0.26	87.96 ± 0.33	316.72	5.08	IC 190629A	-20.693
FRB 20190622A	58656.407	297.77 ± 0.23	85.81 ± 0.29	1122.84	1.28	IC 190629A	-7.4014
FRB 20190625C	58659.775	73.29 ± 0.21	11.10 ± 0.05	442.17	4.41	IC 190712A	-16.277
FRB 20190630C	58664.743	67.91 ± 0.21	80.96 ± 0.09	1660.25	1.85	IC 190629A	0.93471
FRB 20190701B	58665.410	302.51 ± 0.22	80.17 ± 0.24	749.15	2.18	IC 190629A	1.6017
FRB 20190702C	58666.281	284.58 ± 0.27	88.75 ± 0.30	1560.94	3.87	IC 190629A	2.4728
FRB 20190713B	58677.967	159.85 ± 0.21	26.48 ± 0.07	416.06	1.09	IC 190704A	9.1832
FRB 20190722B	58686.703	41.09 ± 0.18	88.97 ± 0.13	508.43	6.84	IC 190629A	22.894
FRB 20200623B	59023.295	257.34 ± 0.24	26.24 ± 0.26	259.6	—	IC 200530A	23.965
FRB 20200813B	59074.588	54.56 ± 0.21	36.34 ± 0.21	221.06	1.20	IC 200911A	-29.009
FRB 20201010A	59132.793	185.62 ± 0.22	33.73 ± 0.23	1333.88	12.88	IC 200926B	13.852

NOTE—We list FRB name, detection epoch (MJD), CHIME right ascension and declination with 1σ uncertainties, dispersion measure (`dm_fitb`), fluence, associated neutrino event, and time gap. Positive time gaps indicate FRBs detected after the corresponding neutrino alert; negative values indicate FRBs detected before the alert.

Table 2. Properties of IceCube events associated with at least one pair in Table 1

Event name	MJD	I3type	RA	Dec	Energy	FAR	Signalness
			(deg)	(deg)	(TeV)	(/year)	(%)
IC 190317A	58559.8	gfu-bronze	81.25 ^{+5.89} _{-5.98}	3.21 ^{+3.93} _{-4.4}	108.0	4.4	26
IC 190629A	58663.8	gfu-bronze	29.12 ^{+39.68} _{-118.65}	84.56 ^{+4.66} _{-4.07}	109.0	0.64	34.3
IC 190704A	58668.8	gfu-bronze	161.81 ^{+2.15} _{-3.91}	26.9 ^{+1.94} _{-1.91}	155.0	1.00	48.6
IC 190712A	58676.1	gfu-bronze	76.64 ^{+5.23} _{-6.99}	12.75 ^{+4.79} _{-2.82}	109.0	2.61	30.4
IC 200530A	58999.3	ehe-gold	255.37 ^{+2.46} _{-2.55}	26.61 ^{+2.32} _{-3.25}	82.0	1.95	59.0
IC 200911A	59103.6	gfu-bronze	51.11 ^{+4.39} _{-10.99}	38.11 ^{+2.31} _{-1.97}	110.0	0.97	40.8
IC 200926B	59118.9	gfu-bronze	184.75 ^{+3.65} _{-1.54}	32.93 ^{+1.16} _{-0.88}	121.0	1.29	43.4

NOTE—For each neutrino alert, we list event name, trigger epoch, alert stream class (I3type), reconstructed coordinates with asymmetric 90% containment uncertainties, estimated energy, false-alarm rate (FAR), and signalness (astrophysical probability).

detection by CHIME/FRB within a given two-sided time window $|\Delta T|$ before and after a neutrino detection.

$$P_T(\Delta T) = 1 - \exp(-\lambda), \quad (1)$$

where λ is the expected number of FRBs detected by CHIME/FRB within a time offset ΔT . We define the time offset between the FRB and neutrino detection as $\Delta T \equiv T_{\text{FRB}} - T_\nu$, where positive (negative) values indicate FRBs detected after (before) the neutrino

event. For FRB 20190630C–IC 190629A, we therefore use $\Delta T = +0.93$ days.

As the detection rate of non-repeating FRBs is not a uniform distribution over the search duration, especially the gap between 2018 and 2019 is outstanding, we derive an average CHIME/FRB detection rate, R_{FRB} , for a short period of 30 days and adopt a value according to the neutrino detection time (Fig. 1). The expected number of FRBs, λ , occurring within a time window of $2|\Delta T|$ is then given by:

$$\lambda = 2|\Delta T|R_{\text{FRB}}, \quad (2)$$

where R_{FRB} is the daily FRB detection rate derived from the Second CHIME/FRB Catalogue, and the factor of 2 reflects the use of a two-sided temporal window. For example, in the case of IC 190629A, we obtain the detection rate, $R_{\text{FRB}} = 1.5$ FRBs day⁻¹ (Fig. 1), and the expected number of non-repeating FRBs occurring within a symmetric ± 0.93 -day time window, $\lambda = 2.79$, respectively. As a result, the probability of a chance temporal coincidence is provided as below:

$$P_{\text{T}}(0.93 \text{ day}) = 1 - \exp(-2.79) \simeq 0.94. \quad (3)$$

While non-repeating FRBs follow a Poisson process, where bursts occur independently and at a constant average rate, the periodic or bursty activity of repeating FRBs deviates from the randomness of a Poisson process as the bursts tend to cluster or exhibit regular cycles (The CHIME/FRB Collaboration et al. 2020b; K. M. Rajwade et al. 2020). Disregarding the non-Poissonian nature of repeating FRBs, we derive $R_{\text{FRB}} = 1.8$ FRBs day⁻¹ and $\lambda = 3.4$ for all CHIME FRBs including repeating FRBs, respectively, which produces a conservative probability of $P_{\text{T}}(0.93 \text{ day}) \simeq 0.96$.

Using the first CHIME baseband catalogue improves the temporal probability to $P_{\text{T}}(0.93 \text{ day}) = 0.76$ with $R_{\text{FRB}} = 0.78$ FRBs day⁻¹ and $\lambda = 1.4$ for non-repeating FRBs, and $P_{\text{T}}(0.93 \text{ day}) = 0.82$ with $R_{\text{FRB}} = 0.93$ FRBs day⁻¹ and $\lambda = 1.7$ when including repeating FRBs.

For comparison, adopting a one-sided temporal window, which assumes a specific time ordering between the FRB and neutrino, yields $P_{\text{T}} \simeq 0.75$ (cf. $P_{\text{T}} \simeq 0.94$ for the two-sided case) for the adopted time offset ($\Delta T = 0.93$ days). Across the different analysis setups (e.g., catalogue selection and treatment of repeating FRBs), this corresponds to a change of only 20–50% and thus does not significantly affect the overall probability.

3.2. Probability of a chance spatial coincidence P_{S}

The probability of a chance spatial coincidence, P_{S} , represents the likelihood that the CHIME/FRB telescope would, purely by chance, detect a non-repeating FRB within the 90% credible localization region of a given neutrino event. We define P_{S,ν_i} as the fraction of all non-repeating FRBs detected by CHIME/FRB that fall within the 90% localization region of the neutrino event ν_i :

$$P_{\text{S},\nu_i} = \frac{N_{\text{FRB},\nu_i}}{N_{\text{FRB},\text{total}}}, \quad (4)$$

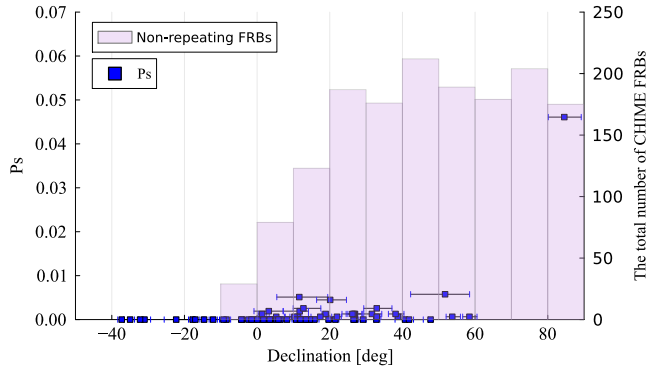


Figure 2. Declination dependencies of the spatial chance coincidence, P_{S} (blue squares; left vertical axis), and the total number of CHIME FRBs (magenta histogram; right vertical axis). The horizontal error bars on the blue squares indicate the positional uncertainty in declination for each neutrino event.

where N_{FRB,ν_i} is the number of non-repeating FRBs within the 90% credible localization region of ν_i , and $N_{\text{FRB},\text{total}}$ is the total number of non-repeating FRBs detected over the whole sky. This definition corresponds to a simple coverage fraction within each localization region, rather than a localization-PDF-weighted statistic, and thus provides an empirical estimate of the probability of a spatial coincidence under the null hypothesis of no physical association.

For the neutrino event IC 190629A, 72 out of 1562 non-repeating FRBs in the CHIME/FRB catalogue are located within its 90% credible localization region, yielding $P_{\text{S}} = 0.047$. Using the first CHIME/FRB baseband catalogue instead, the estimated probability decreases to $P_{\text{S}} = 0.025$ and 0.029 when excluding and including repeating FRBs, respectively.

The detection rate of FRBs by CHIME/FRB is strongly dependent on declination, with a higher incidence at larger declinations due to the telescope’s sensitivity pattern. This introduces an observational bias, whereby apparent correlations between FRBs and neutrinos could be driven by the non-uniform sky coverage rather than a genuine physical association. To account for this, the definition of P_{S} implicitly includes CHIME/FRB’s declination-dependent sensitivity, as it is calculated from the full FRB population observed under actual sky exposure conditions. As shown in Fig. 2, the distribution of P_{S} accurately reflects the telescope’s observational cadence and sky coverage, allowing us to differentiate physical associations from spurious coincidences arising from geometric or instrumental biases.

Following A. Moroiianu et al. (2022), the probability of a chance association for the i -th neutrino event is described as the product of $P_{\text{T}}(\Delta T)$ and P_{S,ν_i} :

$$p[\text{FRB}|\nu_i, \Delta T] = P_T(\Delta T) P_{S,\nu_i}. \quad (5)$$

The resulting chance probabilities $p[\text{FRB}|\nu_i, \Delta T]$ for the association between FRBs and neutrinos with $\Delta T = 0.93$ days are listed in Table 3. However, such coincidences can arise purely by chance when a large number of independent trials are performed. For instance, testing multiple neutrino events against many FRBs increases the likelihood of spurious associations, i.e., the look-elsewhere effect. Therefore, in the next section, we account for the look-elsewhere effect to avoid overestimating the statistical significance.

3.3. Probability of a chance association between FRBs and neutrinos $p[\text{FRB}|\nu, \Delta T]$

We estimate the probability of a chance association between FRBs and neutrinos under the null hypothesis that the two populations are unrelated and distributed independently in time and sky position. Under this assumption, the probability follows a Poisson distribution. The p -value for detecting at least one such coincident event by chance is given by:

$$p[\text{FRB}|\nu, \Delta T] = 1 - \exp(-\langle N \rangle), \quad (6)$$

where $\langle N \rangle$ is the expected number of random coincidences across all 73 neutrino events defined as follows:

$$\langle N \rangle = \sum_{i=1}^{73} p[\text{FRB}|\nu_i, \Delta T]. \quad (7)$$

Under the null hypothesis, individual neutrino alerts are treated as independent trials, and the expected number of chance coincidences is given by $\langle N \rangle = \sum_i p_i$.

Table 4 summarizes the chance-coincidence probabilities for the most significant FRB–neutrino pair at $\Delta T = 0.93$ days, including the trial correction. In our primary analysis based on non-repeating FRBs from the Second CHIME/FRB catalogue, we obtain $p[\text{FRB}|\nu, \Delta T] = 0.076$ (1.43σ), indicating no statistically significant association. Repeating FRBs are excluded from the primary analysis because their burst occurrence is non-Poissonian (e.g., clustered or periodic), but alternative catalogue/repeater choices give consistent conclusions, with all cases remaining below 2σ (Table 4).

To quantify the timescale implied by this null result, we repeat the same $p[\text{FRB}|\nu, \Delta T]$ calculation while scanning the coincidence window $|\Delta T|$ from longer to shorter values. For each trial value of ΔT , we evaluate Equations (6) and (7) and convert $p[\text{FRB}|\nu, \Delta T]$ into a one-sided Gaussian-equivalent significance. We define $|\Delta T_{3\sigma}| \sim 256$ s and $|\Delta T_{5\sigma}| \sim 63$ ms as the windows at

Table 3. Single-event chance-probability for the most significant candidate pair, FRB 20190630C–IC 190629A, using a two-sided time window

Catalogue	Repeater	P_T	P_S	$p[\text{FRB} \nu_i, \Delta T]$
2nd-Intensity	Excluded	0.94	0.046	0.044
2nd-Intensity	Included	0.96	0.047	0.045
1st-Baseband	Excluded	0.76	0.025	0.019
1st-Baseband	Included	0.82	0.029	0.024

Table 4. Trial-corrected chance probabilities for FRB–neutrino pairs within a two-sided ± 0.93 day time window

Catalogue	Repeater	$p[\text{FRB} \nu, \Delta T]$	Significance
2nd-Intensity	Excluded	0.076	1.43σ
2nd-Intensity	Included	0.074	1.44σ
1st-Baseband	Excluded	0.038	1.77σ
1st-Baseband	Included	0.042	1.73σ

which the trial-corrected probability reaches the corresponding thresholds. Within this null-hypothesis framework, the data are consistent with chance coincidences; therefore, any genuine FRB–neutrino association would be required to occur on timescales shorter than these limits.

4. UPPER LIMIT ON NEUTRINO / RADIO LUMINOSITY RATIO

In this section, we derive population-level upper limits on the neutrino-to-radio luminosity ratio, ξ , from the non-detection of statistically significant FRB–neutrino associations. The parameter ξ was first introduced by S. Yamasaki et al. (2016) in the context of GeV gamma-ray counterpart analyses. The analysis uses FRB observables from the Second CHIME/FRB catalogue, including dispersion measure (DM), burst fluence (Jy ms), sky position, and effective bandwidth (MHz). Section 4.1 converts DM into redshift for distance and energetics calculations following T. Hashimoto et al. (2020, 2022). We estimate the intergalactic contribution, DM_{IGM} , using Equation (2) of B. Zhou et al. (2014) with the adopted cosmological assumptions. In our analysis, we assume a standard Λ CDM cosmology ($\Omega_m = 0.3111$, $\Omega_\Lambda = 0.6889$, $\Omega_b = 0.04897$, $h = 0.6766$). Section 4.2 defines the source-frame neutrino-to-radio luminosity ratio and links it to observable FRB and neutrino quantities. Section 4.3 then computes the stacked expected neutrino counts and derives 90% confidence upper limits on ξ for neutrino spectral indices $\gamma = 1.0 - 3.0$.

4.1. Conversion from dispersion measure into redshift

For each FRB, we estimate redshift z from the observed DM following T. Hashimoto et al. (2020, 2022). This approach has been validated against FRBs with spectroscopic host redshifts and is consistent within the reported uncertainties (T. Hashimoto et al. 2020). We decompose the observed DM into Milky Way interstellar, Milky Way halo, intergalactic, and host-galaxy contributions,

$$\text{DM}_{\text{obs}} = \text{DM}_{\text{MW}} + \text{DM}_{\text{halo}} + \text{DM}_{\text{IGM}}(z) + \frac{\text{DM}_{\text{host}}}{1+z}, \quad (8)$$

where DM_{MW} is taken from Galactic electron-density models (NE2001; J. M. Cordes & T. J. W. Lazio 2002 and YMW16; J. M. Yao et al. 2017), $\text{DM}_{\text{halo}} = 30 \text{ pc cm}^{-3}$ (e.g. S. Yamasaki & T. Totani 2020; A. M. Cook et al. 2023; F. Collaboration et al. 2026), and $\text{DM}_{\text{host}} = 50 \text{ pc cm}^{-3}$ (J.-P. Macquart et al. 2020; T. Hashimoto et al. 2022). We adopt the fixed values of DM_{halo} and DM_{host} following previous studies, and these should be regarded as empirical assumptions rather than parameters derived in this work. The intergalactic contribution $\text{DM}_{\text{IGM}}(z)$ is computed using the cosmological prescription of B. Zhou et al. (2014). We perform the DM– z conversion using both NE2001- and YMW16-based DM_{MW} estimates, and present the corresponding upper-limit results separately in Table 5. Under these assumptions, Equation (8) is solved numerically for each burst to obtain $z_i = z(\text{DM}_{\text{obs},i})$, which is used in the luminosity-distance and energetics calculations below. The resulting redshift distribution for the CHIME sample has a mean of $\langle z \rangle \sim 0.53$ with a dispersion of $\sigma_z \sim 0.47$. We note that the DM-based redshift estimate itself has substantial systematic uncertainty; for typical CHIME FRBs, the uncertainty is of order $\Delta z \sim 0.1$ (T. Hashimoto et al. 2022). These DM– z systematics, including uncertainties in DM_{halo} and DM_{host} , are not propagated into the present ξ upper-limit calculation; therefore, the reported limits should be interpreted within the adopted fiducial DM decomposition.

4.2. Neutrino-radio luminosity ratio

To set upper limits on FRB physical quantities from the non-detection of neutrinos, we define the neutrino-to-radio luminosity ratio in the source rest frames as

$$\xi \equiv \frac{(\nu L_\nu)_\nu^{\text{src}}}{(\nu L_\nu)_{\text{FRB}}^{\text{src}}} = \frac{E_\nu^{\text{iso}}}{E_{\text{FRB}}^{\text{iso}}} \times \frac{\Delta t_{\text{FRB}}}{\Delta t_\nu}, \quad (9)$$

where $(\nu L_\nu)_\nu^{\text{src}}$ and $(\nu L_\nu)_{\text{FRB}}^{\text{src}}$ are the source-frame spectral luminosities per logarithmic energy/frequency interval (i.e., νL_ν) of the neutrino and FRB emission,

respectively. Here E_ν^{iso} and $E_{\text{FRB}}^{\text{iso}}$ denote the neutrino and FRB source-frame isotropic-equivalent energies, and Δt_ν and Δt_{FRB} are their intrinsic emission durations. Equation (9) follows from $(\nu L_\nu) \propto E^{\text{iso}}/\Delta t$ and is connected to observables through the redshift conversion described below. For each i -th FRB, the isotropic FRB radio energy

$$E_{\text{FRB},i}^{\text{iso}}(z_i) = 4\pi D_L^2(z_i) \frac{\mathcal{F}_{\text{FRB},i}^{\text{obs}}}{1+z_i}, \quad (10)$$

where $D_L(z_i)$ is the luminosity distance and $\mathcal{F}_{\text{FRB},i}^{\text{obs}}$ is the band-integrated radio energy fluence (erg cm^{-2}). The observer-frame and source-frame fluence are related by $\mathcal{F}^{\text{src}} = (1+z)\mathcal{F}^{\text{obs}}$. For each FRB, we use the burst fluence density $\mathcal{F}_{\nu,\text{FRB},i}^{\text{obs}}$ (Jy ms), sky position, effective bandwidth $\Delta\nu$ (MHz), and DM (pc cm^{-3}) from the Second CHIME/FRB catalogue. We compute $\mathcal{F}_{\text{FRB},i}^{\text{obs}} = \Delta\nu \mathcal{F}_{\nu,\text{FRB},i}^{\text{obs}}$ and estimate redshift from DM as described in Section 4.1.

In this analysis, we adopt a single effective neutrino-to-radio luminosity ratio, ξ , for the FRB population, i.e. a common ξ for all FRBs. This should be interpreted as a population-averaged effective parameter, not as evidence that all individual FRBs share identical intrinsic ξ . We then model the source-frame neutrino spectrum as a power law, $dL_\nu/d\epsilon_\nu \propto \epsilon_\nu^{-\gamma}$, where $dL_\nu/d\epsilon_\nu$ denotes the differential neutrino luminosity per unit neutrino particle energy ϵ . In general, a radio K -correction factor, $K(z_i)$, is required to account for cosmological redshift when converting from the observer-frame to the source rest frame. In radio astronomy, assuming a power-law spectrum $S_\nu \propto \nu^{-\alpha}$, the K -correction is typically expressed as $K(z_i) = (1+z_i)^{\alpha-1}$. Because our sample is concentrated at low redshift ($z \lesssim 1.2$ for 90% of the sample), the radio K -correction can change the inferred energetics by up to a factor of two for plausible spectral indices $\alpha = 0-2$. We therefore neglect the K -correction in this analysis.

To account for the current uncertainty in the FRB neutrino-emission mechanism, we evaluate a grid of spectral indices, $\gamma = 1.0, 1.5, 2.0, 2.5$, and 3.0 . This range is chosen to bracket plausible hard-to-soft spectral behaviors, from efficient particle acceleration scenarios—such as diffusive shock acceleration, which typically yields $\gamma \sim 2$ —to cases where radiative cooling, particle escape, or transport effects lead to softer, steeper spectra with $\gamma \gtrsim 2.5-3$ (e.g., J. K. Becker 2008; N. Kurahashi et al. 2022).

4.3. Upper limit on the neutrino-radio luminosity ratio

The expected number of neutrinos detected from an i -th FRB at declination δ_i and redshift z_i is

$$\lambda_i(\xi, \delta_i, z_i) = \int_{\epsilon_{\nu, \min}^{\text{obs}}}^{\epsilon_{\nu, \max}^{\text{obs}}} d\epsilon_{\nu}^{\text{obs}} \frac{A_{\text{eff}}(\epsilon_{\nu}^{\text{obs}}, \delta_i)}{\epsilon_{\nu}^{\text{obs}}} \frac{d\mathcal{F}_{\nu, i}^{\text{obs}}(\epsilon_{\nu}^{\text{obs}}; z_i, \xi)}{d\epsilon_{\nu}^{\text{obs}}}, \quad (11)$$

where $A_{\text{eff}}(\epsilon_{\nu}^{\text{obs}}, \delta_i)$ is the IceCube effective area for the muon-neutrino channel ($\nu_{\mu} + \bar{\nu}_{\mu}$) as a function of observed neutrino energy $\epsilon_{\nu}^{\text{obs}}$ and declination δ_i , and $\mathcal{F}_{\nu, i}^{\text{obs}}(\epsilon_{\nu}^{\text{obs}}; z_i, \xi)$ is the neutrino energy fluence (time-integrated energy flux) in units of erg cm^{-2} , derived from equations (9) and (10). We use the IceCube effective area for the GFU Gold and Bronze alert selections reported in ICECAT1 (R. Abbasi et al. 2023b); this A_{eff} includes the corresponding alert-selection response (trigger, reconstruction, and quality cuts). For each i -th FRB, we compute the expected number of neutrinos by integrating over 1 TeV to 1 PeV, following previous work (S. Fahey et al. 2017; A. Albert et al. 2018; M. G. Aartsen et al. 2018; R. Abbasi et al. 2023a).

Therefore, the total expected neutrino counts from all FRBs can be calculated as

$$N(\xi) = \sum_{i=1}^{N_{\text{FRB}}} \lambda_i(\xi, \delta_i). \quad (12)$$

The expected number $N(\xi)$ increases with increasing ξ because a higher neutrino-to-radio luminosity ratio yields a higher detectable neutrino fluence. With zero neutrino detections, we derive the 90% upper limit ξ_{90} by requiring $N(\xi_{90}) = -\ln(0.1) \simeq 2.30$, which corresponds to the one-sided 90% Poisson upper limit on the expected mean for zero observed events. For the temporal normalization, we assume that the neutrino-emitting duration is equal to the FRB duration reported in the Second CHIME/FRB catalogue, so that the time-integrated neutrino fluence is evaluated over the same emission interval. If the true neutrino duration lies within the range of 0.1–1000 s predicted by B. D. Metzger et al. (2020), our upper limits could improve by up to about five orders of magnitude.

Table 5 summarizes the upper limits on the neutrino-to-radio energy ratio, adopting NE2001 as our fiducial Galactic electron-density model (J. M. Cordes & T. J. W. Lazio 2002; S. K. Ocker & J. M. Cordes 2026). We also repeated the same analysis with YMW16 (J. M. Yao et al. 2017) and found nearly identical upper limits for all spectral indices, indicating negligible model dependence in this work. For reference, we translate these limits into order-of-magnitude constraints on the isotropic neutrino energy by adopting a typical FRB isotropic radio energy of $E_{\text{FRB, typ}}^{\text{iso}} \sim 10^{38-41}$ erg (e.g., T. Hashimoto et al. 2022; K. Shin et al. 2023; L. Tang et al. 2023), yielding $E_{\nu, 90}^{\text{iso}} \sim \xi_{90} E_{\text{FRB, typ}}^{\text{iso}}$. The derived

Table 5. The 90 % upper limits on the neutrino-to-radio luminosity ratio, ξ_{90} , and corresponding order-of-magnitude isotropic neutrino-energy estimates

γ	$\xi_{\text{NE2001, 90}}$	$E_{\nu, 90}^{\text{iso}}$ (erg)
1.0	4.1×10^8	$\sim 10^{46-49}$
1.5	1.6×10^9	$\sim 10^{47-50}$
2.0	9.3×10^9	$\sim 10^{47-50}$
2.5	5.9×10^{10}	$\sim 10^{48-51}$
3.0	3.6×10^{11}	$\sim 10^{49-52}$

upper limits of $\xi \lesssim 10^8 - 10^{11}$ with neutrino spectral indices of $\gamma = 1.0 - 3.0$ represent an improvement of approximately two orders of magnitude compared to the most stringent constraint reported in the previous studies based on limited FRB samples (e.g., M. G. Aartsen et al. 2020).

5. DISCUSSION AND CONCLUSION

In this paper, we searched for temporal and spatial coincidences between FRBs in the Second CHIME/FRB catalogue and high-energy neutrinos in ICECAT1. After accounting for the declination-dependent CHIME/FRB exposure and the look-elsewhere effect associated with multiple-event trials, we find no statistically significant FRB–neutrino association. Within the present null-hypothesis framework and trial treatment, a detectable association corresponds to time offsets shorter than approximately 256 s (3σ) or 63 ms (5σ).

The most significant coincidence is found between FRB 20190630C and IC 190629A, where the FRB occurred 0.93 days after the neutrino detection within the 90% localization region. However, the post-trial probability of this coincidence is $p = 0.076$ (1.43σ), indicating that it is consistent with a chance association. Therefore, our analysis finds no compelling evidence for neutrino emission associated with FRBs in the current datasets. Our primary significance estimate is based on the two-sided (order-agnostic) temporal hypothesis. For comparison, one-sided hypotheses (FRB-after-neutrino only and FRB-before-neutrino only) also yield non-significant associations and do not alter our main conclusion. Thus, the present data do not provide evidence for a preferred emission ordering between FRBs and high-energy neutrinos.

Despite the absence of significant detections, this study provides new constraints on neutrino production in FRBs. We derive upper limits on the neutrino-to-radio luminosity ratio of $\xi \lesssim 10^8 - 10^{11}$ for neutrino spectral indices $\gamma = 1.0, 1.5, 2.0, 2.5,$ and 3.0 (see Table 5), representing the most stringent constraints to date from FRB–neutrino coincidence searches within the assump-

tions adopted in this work. These limits improve upon the previously reported most stringent constraints by approximately two orders of magnitude, based on studies with limited FRB samples (e.g., [M. G. Aartsen et al. 2020](#)). For reference, adopting a typical FRB isotropic radio energy of $E_{\text{FRB}}^{\text{iso}} \sim 10^{38-41}$ erg, these limits correspond to order-of-magnitude constraints on isotropic neutrino energies of 10^{46-52} erg for neutrino spectral indices $\gamma = 1.0 - 3.0$.

For comparison, the Galactic FRB 20200428D from the magnetar SGR 1935+2154 yields a more stringent event-level constraint on the neutrino-to-radio luminosity ratio ($\xi \lesssim 10^7$; [B. D. Metzger et al. 2020](#)), primarily because of its very small distance (~ 10 kpc). However, this limit is derived from a single Galactic magnetar flare and therefore does not necessarily represent the neutrino-emission properties of the cosmological FRB population. By contrast, our non-detection between the Second CHIME/FRB Catalogue and ICECAT1 constrains the population-averaged neutrino emissions of cosmological FRBs through the absence of temporally and spatially coincident events. Although the Galactic constraint is stronger, the two limits probe physically distinct regimes. In particular, FRB 20200428D has a radio energy of $E_{\text{radio}} \sim 10^{34}$ erg, several orders of magnitude below typical cosmological FRBs. This difference suggests that the burst energetics or emission environments may differ between the Galactic event and cosmological FRBs, and therefore the neutrino production efficiency inferred from FRB 20200428D cannot be directly extrapolated to the cosmological FRB population.

These limits can be compared with theoretical expectations for neutrino emission from FRB progenitors. For example, models based on synchrotron maser shocks in magnetar-driven blast waves predict total neutrino energies in the range of 10^{35-44} erg occurring within seconds of the FRB ([B. D. Metzger et al. 2020](#)). While our current limits remain several orders of magnitude above the predictions of most magnetar-based FRB models, they begin to constrain scenarios invoking unusually energetic hadronic outflows.

Future observational capabilities can improve two distinct goals: (i) the discovery of physically associated FRB–neutrino events and (ii) tighter population-level upper limits on the neutrino-to-radio luminosity ratio derived from non-detections. For event-level association searches, the primary limitation in the present analysis is the modest angular resolution of track-like neutrino events (typically a few degrees), which increases the spatial chance-coincidence term in Equation (4) and degrades the final chance probability in Equation (6). The currently limited sample of nearby bright FRBs further

reduces the chance of detecting true associations at the present detector sensitivity. A practical improvement is to prioritize well-localized track-like neutrino events (angular uncertainty of less than 1° ; [M. G. Aartsen et al. 2014](#)), which can significantly suppress spatial chance coincidences. On the detector side, IceCube-Gen2 is expected to provide an effective area approximately five times larger than IceCube, implying a comparable improvement in FRB–neutrino search efficiency ([G. Collaboration et al. 2014](#); [M. G. Aartsen et al. 2021](#)).

For population-level constraints, testing magnetar-flare scenarios such as [B. D. Metzger et al. \(2020\)](#) and [Y. Qu & B. Zhang \(2022\)](#) requires substantially larger samples of nearby bright FRBs so that non-detections translate into tighter limits on the neutrino-to-radio luminosity ratio. In this context, ultra-wide-field surveys such as the Bustling Universe Radio Survey Telescope in Taiwan (BURSTT; [H.-H. Lin et al. 2022](#); [D. F.-J. Ling et al. 2023](#); [K.-Y. Lin et al. 2025](#)) and the CHIME/FRB outriggers ([A. E. Lanman et al. 2024](#); [F. Collaboration et al. 2025](#)) are particularly promising. With a field of view up to ~ 50 times that of CHIME/FRB and a design optimized for nearby bright FRBs, BURSTT may improve the efficiency of constructing nearby FRB samples by nearly an order of magnitude. Combined with improved neutrino localization and higher neutrino sensitivity, future population-level stacking analyses could tighten the upper limits on ξ by up to ~ 2 orders of magnitude. Further improvement also requires reducing systematic uncertainties in DM-based distance estimates and in the assumed neutrino-emission duration.

In addition to increasing nearby FRB samples, deep interferometric surveys with next-generation arrays—including the Square Kilometer Array (SKA; [P. E. Dewdney et al. 2009](#); [T. Bourke et al. 2018](#); [R. Braun et al. 2019](#); [A. Weltman et al. 2020](#)) and the Deep Synoptic Array (DSA-2000) ([A. Tiwary et al. 2024](#))—may uncover faint or strongly scattered bursts that are missed by current instruments. This possibility is particularly relevant if a subset of FRBs resides in dense environments (e.g., [B. D. Metzger et al. 2020](#)), where free-free absorption or induced Compton scattering can suppress the observable radio flux even when particle acceleration (and possible neutrino production) remains active. Together with next-generation neutrino detectors, such searches provide a complementary route to test FRB–neutrino connections in otherwise radio-obscured source populations.

ACKNOWLEDGMENTS

This study was supported by JST SPRING (JP-MJSP2108), and International Graduate Program for Excellence in Earth-Space Science (IGPEES), a World-leading Innovative Graduate Study (WINGS) Program, the University of Tokyo, and International Internship Pilot Program (IIPP), provided by the National Science and Technology Council (NSTC) in Taiwan. We also gratefully acknowledge the CHIME/FRB Collaboration and the IceCube Collaboration for providing the high-quality catalogs essential to this research. Their efforts and open data sharing have been invaluable to the advancement of our work. TH acknowledges the sup-

port of the National Science and Technology Council of Taiwan (NSTC) through grants 113-2112-M-005-009-MY3, 113-2123-M-001-008-, and 111-2112-M-005-018-MY3 and the Ministry of Education of Taiwan through the grant 113RD109. SY acknowledges the support from the NSTC through grant numbers 113-2112-M-005-007-MY3 and 113-2811-M-005-006-. This work is supported by the Grants-in-Aid for Scientific Research Nos. 25KJ0024, 25K17378 (T.W.) from the Ministry of Education, Culture, Sports, Science and Technology (MEXT) of Japan.

REFERENCES

- Aartsen, M., Ackermann, M., Adams, J., et al. 2018a, *Science*, 361, doi: [10.1126/science.aat1378](https://doi.org/10.1126/science.aat1378)
- Aartsen, M., Ackermann, M., Adams, J., et al. 2018b, *Science*, 361, 147–151, doi: [10.1126/science.aat2890](https://doi.org/10.1126/science.aat2890)
- Aartsen, M. G., Abbasi, R., Ackermann, M., et al. 2014, *Journal of Instrumentation*, 9, P03009, doi: [10.1088/1748-0221/9/03/P03009](https://doi.org/10.1088/1748-0221/9/03/P03009)
- Aartsen, M. G., Ackermann, M., Adams, J., et al. 2018, *The Astrophysical Journal*, 857, 117, doi: [10.3847/1538-4357/aab4f8](https://doi.org/10.3847/1538-4357/aab4f8)
- Aartsen, M. G., Ackermann, M., Adams, J., et al. 2020, *The Astrophysical Journal*, 890, 111, doi: [10.3847/1538-4357/ab564b](https://doi.org/10.3847/1538-4357/ab564b)
- Aartsen, M. G., Abbasi, R., Ackermann, M., et al. 2021, *Journal of Physics G: Nuclear and Particle Physics*, 48, 060501, doi: [10.1088/1361-6471/abbd48](https://doi.org/10.1088/1361-6471/abbd48)
- Abbasi, R., Ackermann, M., Adams, J., et al. 2022, *Science*, 378, 538, doi: [10.1126/science.abg3395](https://doi.org/10.1126/science.abg3395)
- Abbasi, R., Ackermann, M., Adams, J., et al. 2023a, *The Astrophysical Journal*, 946, 80, doi: [10.3847/1538-4357/acbea0](https://doi.org/10.3847/1538-4357/acbea0)
- Abbasi, R., Ackermann, M., Adams, J., et al. 2023b, *The Astrophysical Journal Supplement Series*, 269, 25, doi: [10.3847/1538-4365/acfa95](https://doi.org/10.3847/1538-4365/acfa95)
- Abbott, B. P., Abbott, R., Abbott, T. D., et al. 2020, *The Astrophysical Journal Letters*, 892, L3, doi: [10.3847/2041-8213/ab75f5](https://doi.org/10.3847/2041-8213/ab75f5)
- Albert, A., André, M., Anghinolfi, M., et al. 2018, *Monthly Notices of the Royal Astronomical Society*, 482, 184, doi: [10.1093/mnras/sty2621](https://doi.org/10.1093/mnras/sty2621)
- Becker, J. K. 2008, *PhR*, 458, 173, doi: [10.1016/j.physrep.2007.10.006](https://doi.org/10.1016/j.physrep.2007.10.006)
- Bochenek, C. D., Ravi, V., Belov, K. V., et al. 2020, *Nature*, 587, 59, doi: [10.1038/s41586-020-2872-x](https://doi.org/10.1038/s41586-020-2872-x)
- Bourke, T., Braun, R., Bonaldi, A., et al. 2018, in *American Astronomical Society Meeting Abstracts*, Vol. 231, American Astronomical Society Meeting Abstracts #231, 152.07
- Braun, R., Bonaldi, A., Bourke, T., Keane, E., & Wagg, J. 2019, *Anticipated Performance of the Square Kilometre Array – Phase 1 (SKA1)*, <https://arxiv.org/abs/1912.12699>
- Bustamante, M., Ellis, J., Konoplich, R., & Sakharov, A. S. 2024, *Probing Lorentz invariance with a high-energy neutrino flare*, <https://arxiv.org/abs/2408.15949>
- Collaboration, F., Amiri, M., Amouyal, D., et al. 2025, *A Catalog of Local Universe Fast Radio Bursts from CHIME/FRB and the KKO Outrigger*, <https://arxiv.org/abs/2502.11217>
- Collaboration, F., Abbott, T., Andersen, B. C., et al. 2026, *The Second CHIME/FRB Catalog of Fast Radio Bursts*, <https://arxiv.org/abs/2601.09399>
- Collaboration, G., Aartsen, M. G., Ackermann, M., et al. 2014, *IceCube-Gen2: A Vision for the Future of Neutrino Astronomy in Antarctica*, <https://arxiv.org/abs/1412.5106>
- Cook, A. M., Bhardwaj, M., Gaensler, B. M., et al. 2023, *The Astrophysical Journal*, 946, 58, doi: [10.3847/1538-4357/acbbd0](https://doi.org/10.3847/1538-4357/acbbd0)
- Cordes, J. M., & Lazio, T. J. W. 2002, *arXiv e-prints*, astro, doi: [10.48550/arXiv.astro-ph/0207156](https://doi.org/10.48550/arXiv.astro-ph/0207156)
- DeLaunay, J. J., Fox, D. B., Murase, K., et al. 2016, *The Astrophysical Journal Letters*, 832, L1, doi: [10.3847/2041-8205/832/1/11](https://doi.org/10.3847/2041-8205/832/1/11)
- Desai, S. 2022, *Journal of Physics G: Nuclear and Particle Physics*, 50, 015201, doi: [10.1088/1361-6471/aca03b](https://doi.org/10.1088/1361-6471/aca03b)
- Dewdney, P. E., Hall, P. J., Schilizzi, R. T., & Lazio, T. J. L. W. 2009, *IEEE Proceedings*, 97, 1482, doi: [10.1109/JPROC.2009.2021005](https://doi.org/10.1109/JPROC.2009.2021005)

- Fahey, S., Kheirandish, A., Vandenbroucke, J., & Xu, D. 2017, *The Astrophysical Journal*, 845, 14, doi: [10.3847/1538-4357/aa7e28](https://doi.org/10.3847/1538-4357/aa7e28)
- Hashimoto, T., Goto, T., On, A. Y. L., et al. 2020, *Monthly Notices of the Royal Astronomical Society*, 498, 3927, doi: [10.1093/mnras/staa2490](https://doi.org/10.1093/mnras/staa2490)
- Hashimoto, T., Goto, T., Chen, B. H., et al. 2022, *Monthly Notices of the Royal Astronomical Society*, 511, 1961, doi: [10.1093/mnras/stac065](https://doi.org/10.1093/mnras/stac065)
- IceCube Collaboration. 2021, IceCube Data for Neutrino Point-Source Searches Years 2008-2018, IceCube Neutrino Observatory, doi: [10.21234/CPKQ-K003](https://doi.org/10.21234/CPKQ-K003)
- Kurahashi, N., Murase, K., & Santander, M. 2022, *Annual Review of Nuclear and Particle Science*, 72, 365, doi: [10.1146/annurev-nucl-011122-061547](https://doi.org/10.1146/annurev-nucl-011122-061547)
- Lanman, A. E., Andrew, S., Lazda, M., et al. 2024, CHIME/FRB Outriggers: KKO Station System and Commissioning Results, <https://arxiv.org/abs/2402.07898>
- Li, C. K., Lin, L., Xiong, S. L., et al. 2021, *Nature Astronomy*, 5, 378–384, doi: [10.1038/s41550-021-01302-6](https://doi.org/10.1038/s41550-021-01302-6)
- Li, X., Ge, M., Lin, L., et al. 2022, *ApJ*, 931, 56, doi: [10.3847/1538-4357/ac6587](https://doi.org/10.3847/1538-4357/ac6587)
- Lin, H.-H., Lin, K.-y., Li, C.-T., et al. 2022, *PASP*, 134, 094106, doi: [10.1088/1538-3873/ac8f71](https://doi.org/10.1088/1538-3873/ac8f71)
- Lin, K.-Y., Wen, C.-Y., Jiang, H., et al. 2025, Back-End System of BURSTT, <https://arxiv.org/abs/2512.07300>
- Ling, D. F.-J., Hashimoto, T., Yamasaki, S., et al. 2023, *MNRAS*, 518, 1398, doi: [10.1093/mnras/stac3018](https://doi.org/10.1093/mnras/stac3018)
- Lorimer, D. R., Bailes, M., McLaughlin, M. A., Narkevic, D. J., & Crawford, F. 2007, *Science*, 318, 777–780, doi: [10.1126/science.1147532](https://doi.org/10.1126/science.1147532)
- Luo, J.-W., & Zhang, B. 2024, *Monthly Notices of the Royal Astronomical Society*, 534, 70, doi: [10.1093/mnras/stae2071](https://doi.org/10.1093/mnras/stae2071)
- Luszczak, W. 2023, TXS 0506+056 with Updated IceCube Data, <https://arxiv.org/abs/2307.14559>
- Macquart, J.-P., Prochaska, J. X., McQuinn, M., et al. 2020, *Nature*, 581, 391, doi: [10.1038/s41586-020-2300-2](https://doi.org/10.1038/s41586-020-2300-2)
- Mereghetti, S., Savchenko, V., Ferrigno, C., et al. 2020, *ApJL*, 898, L29, doi: [10.3847/2041-8213/aba2cf](https://doi.org/10.3847/2041-8213/aba2cf)
- Metzger, B. D., Fang, K., & Margalit, B. 2020, *The Astrophysical Journal Letters*, 902, L22, doi: [10.3847/2041-8213/abbb88](https://doi.org/10.3847/2041-8213/abbb88)
- Moroianu, A., Wen, L., James, C. W., et al. 2022, An assessment of the Association Between a Fast Radio Burst and Binary Neutron Star Merger, <https://arxiv.org/abs/2212.00201>
- Nicastro, L., Guidorzi, C., Palazzi, E., et al. 2021, *Universe*, 7, doi: [10.3390/universe7030076](https://doi.org/10.3390/universe7030076)
- Ocker, S. K., & Cordes, J. M. 2026, arXiv e-prints, arXiv:2602.11838, doi: [10.48550/arXiv.2602.11838](https://doi.org/10.48550/arXiv.2602.11838)
- Petroff, E., Hessels, J. W. T., & Lorimer, D. R. 2022, *The Astronomy and Astrophysics Review*, 30, doi: [10.1007/s00159-022-00139-w](https://doi.org/10.1007/s00159-022-00139-w)
- Platts, E., Weltman, A., Walters, A., et al. 2019, *Physics Reports*, 821, 1–27, doi: [10.1016/j.physrep.2019.06.003](https://doi.org/10.1016/j.physrep.2019.06.003)
- Qu, Y., & Zhang, B. 2022, *Monthly Notices of the Royal Astronomical Society*, 511, 972, doi: [10.1093/mnras/stac117](https://doi.org/10.1093/mnras/stac117)
- Rajwade, K. M., Mickaliger, M. B., Stappers, B. W., et al. 2020, *Monthly Notices of the Royal Astronomical Society*, 495, 3551, doi: [10.1093/mnras/staa1237](https://doi.org/10.1093/mnras/staa1237)
- Ridnaia, A., Svinkin, D., Frederiks, D., et al. 2021, *Nature Astronomy*, 5, 372, doi: [10.1038/s41550-020-01265-0](https://doi.org/10.1038/s41550-020-01265-0)
- Sharma, A. 2024, *Universe*, 10, doi: [10.3390/universe10080326](https://doi.org/10.3390/universe10080326)
- Shimoda, J., & Wada, T. 2024, arXiv e-prints, arXiv:2409.19915, doi: [10.48550/arXiv.2409.19915](https://doi.org/10.48550/arXiv.2409.19915)
- Shin, K., Masui, K. W., Bhardwaj, M., et al. 2023, *The Astrophysical Journal*, 944, 105, doi: [10.3847/1538-4357/acaf06](https://doi.org/10.3847/1538-4357/acaf06)
- Tang, L., Lin, H.-N., & Li, X. 2023, *Chinese Physics C*, 47, 085105, doi: [10.1088/1674-1137/acda1c](https://doi.org/10.1088/1674-1137/acda1c)
- Tavani, M., Casentini, C., Ursi, A., et al. 2021, *Nature Astronomy*, 5, 401, doi: [10.1038/s41550-020-01276-x](https://doi.org/10.1038/s41550-020-01276-x)
- The CHIME/FRB Collaboration, Andersen, B. C., Bandura, K. M., et al. 2020a, *Nature*, 587, 54, doi: [10.1038/s41586-020-2863-y](https://doi.org/10.1038/s41586-020-2863-y)
- The CHIME/FRB Collaboration, Amiri, M., Andersen, B. C., et al. 2020b, *Nature*, 582, 351, doi: [10.1038/s41586-020-2398-2](https://doi.org/10.1038/s41586-020-2398-2)
- The CHIME/FRB Collaboration, Amiri, M., Andersen, B. C., et al. 2024, *The Astrophysical Journal*, 969, 145, doi: [10.3847/1538-4357/ad464b](https://doi.org/10.3847/1538-4357/ad464b)
- Tiwary, A., Jameson, K., Ravi, V., & Hallinan, G. 2024, in *American Astronomical Society Meeting Abstracts*, Vol. 243, *American Astronomical Society Meeting Abstracts*, 261.26
- Troitsky, S. V. 2021, *Physics-Uspekhi*, 64, 1261, doi: [10.3367/UFNe.2021.09.039062](https://doi.org/10.3367/UFNe.2021.09.039062)
- Weltman, A., Bull, P., Camera, S., et al. 2020, *PASA*, 37, e002, doi: [10.1017/pasa.2019.42](https://doi.org/10.1017/pasa.2019.42)
- Yamasaki, S., & Totani, T. 2020, *ApJ*, 888, 105, doi: [10.3847/1538-4357/ab58c4](https://doi.org/10.3847/1538-4357/ab58c4)
- Yamasaki, S., Totani, T., & Kawanaka, N. 2016, *MNRAS*, 460, 2875, doi: [10.1093/mnras/stw1206](https://doi.org/10.1093/mnras/stw1206)
- Yao, J. M., Manchester, R. N., & Wang, N. 2017, *The Astrophysical Journal*, 835, 29, doi: [10.3847/1538-4357/835/1/29](https://doi.org/10.3847/1538-4357/835/1/29)

Zhang, B. 2024, Annual Review of Nuclear and Particle
Science, 74, 89–112,
doi: [10.1146/annurev-nucl-102020-124444](https://doi.org/10.1146/annurev-nucl-102020-124444)

Zhou, B., Li, X., Wang, T., Fan, Y.-Z., & Wei, D.-M. 2014,
Phys. Rev. D, 89, 107303,
doi: [10.1103/PhysRevD.89.107303](https://doi.org/10.1103/PhysRevD.89.107303)